Fish and Shellfish Immunology 84 (2019) 502–508

Contents lists available at ScienceDirect

Fish and Shellfish Immunology

journal homepage: www.elsevier.com/locate/fsi

Full length article

Novel Ca^{2+}-independent C-type lectin involved in immune defense of the razor clam *Sinonovacula constricta*

Yuhong Shi[a], Xuelin Zhao[a], Zhenhui Wang[a], Yina Shao[a], Weiwei Zhang[a], Yongbo Bao[b,**], Chenghua Li[a,*]

[a] School of Marine Sciences, Ningbo University, Ningbo, 315211, PR China
[b] Zhejiang Key Laboratory of Aquatic Germplasm Resources, Zhejiang Wanli University, Ningbo, 315100, PR China

ARTICLE INFO

Keywords:
Sinonovacula constricta
Bacterial infections
qPCR
Binding activity
Agglutinate activity

ABSTRACT

C-type lectins (CTLs) are important pattern recognition molecules that participate in bacterial binding and agglutination by specific recognition of carbohydrates from pathogens. In this study, a full-length cDNA of CTL was cloned from *Sinonovacula constricta* (designated *ScCTL-2*). *ScCTL*-2 has a length of 981 bp, a 5′-untranslated region (UTR) of 47 bp, a short 3′-UTR of 37 bp, and an open reading frame (ORF) of 894 bp, which encodes a polypeptide of 298 amino acid residues. The deduced amino acid of ScCTL-2 possesses a conserved carbohydrate-recognition domain (CRD) similar to that of C^{31}–E^{171}. Spatial distribution analysis demonstrated that *ScCTL-2* was constitutively expressed in all tested tissues, with dominant expression in foot and siphon and weak expression in hepatopancreas. The mRNA expression level of *ScCTL-2* in gills and hepatopancreas was significantly upregulated at 6 and 12 h after challenge with the pathogen *Vibrio parahaemolyticus*. The recombinant ScCTL-2 showed specific binding and agglutinate capacities to all examined Gram-negative bacterial species, namely, *Escherichia coli*, *Vibro anguillarum*, and *V. parahaemolyticus* in a Ca^{2+}-independent manner. However, these binding activities were not detected in Gram-positive *Micrococcus luteus*. Our results indicated that ScCTL-2 could be a novel pattern recognition receptor that can specifically recognize Gram-negative microorganisms in the innate immunity of *S. constricta*.

1. Introduction

The razor clam *Sinonovacula constricta* is widely distributed in the intertidal zones and estuarine areas of the Western Pacific Ocean and is one of the four marine bivalves produced in China [1,2]. However, bacterial diseases cause high mortality rates and limit the industrial development of the clam [3]. Similar to bivalve mollusks, *S. constricta* lacks adaptive immunity and relies on its innate immune system to defend itself from pathogen infection [4]. Recognition of non-self is the first step of innate immune response, which is mediated by a group of proteins named pattern recognition receptors (PRRs) [5]. Among the 11 identified groups of PRRs in invertebrates, C-type lectins (CTLs) have been the focus of research because of their roles in innate immune responses [6], such as activation of prophenoloxidase [7], regulation of hemocyte phagocytosis [8,9], cell adhesion [10], cell nodulation [11,12], and pathogen elimination [13,14]. CTLs also exhibit food sorting functions [15].

CTLs are a superfamily of Ca^{2+}-dependent carbohydrate-recognition proteins that consist of at least one carbohydrate-recognition domain (CRD), which participate in nonself recognition and clearance of invaders [16]. Among Ca^{2+} binding sites, two conserved motifs determine the binding specificity in the CRD domain in vertebrates [17]. The two motifs in invertebrates are Glu-Pro-Asn (EPN) or Gln-Pro-Asp (QPD) and WND (Trp-Asn-Asp). The former is verified as the key switch in the specificity of binding to carbohydrates, and the latter could increase Ca^{2+} affinity and specificity [18]. Other types of motifs are more abundant in invertebrates than in vertebrates; these motifs include EPN [19–21], Glu-Pro-Asp (EPD) [22], and Gln-Pro-Gly (QPG) [23] in the first motif and Trp-Ser-Asp (WSD) [24] and Trp-His-Asp (WHD) [25] in the second motif. All of these motifs maintain high selectivity for carbohydrate binding by mutation of the motif amino acids [26].

Studies of CTLs in bivalves have focused on identifying carbohydrates as PRRs, particularly the role of lectin in immunity through PAMP, bacterial binding, and agglutination. Yang et al. studied the role of conserved motifs in the recognition of PAMPs through site-directed

* Corresponding author. 818 Fenghua Road, Ningbo University, Ningbo, Zhejiang Province 315211, PR China.
** Corresponding author.
E-mail addresses: bobbao2001@gmail.com (Y. Bao), lichenghua@nbu.edu.cn (C. Li).

https://doi.org/10.1016/j.fsi.2018.10.036
Received 15 May 2018; Received in revised form 6 October 2018; Accepted 14 October 2018
Available online 15 October 2018

mutagenesis [27]. Wang et al. demonstrated that lectin could initiate the cellular adhesion of hemocytes and enhance their encapsulation in vitro [10]. Lectins also act as opsonins to promote phagocytosis in cells [28] and possess antibacterial effects [13]. A recent study reported that lectins could select food particles by identifying carbohydrates [15]. These findings indicate the important role of lectins in shellfish. However, most reported CTLs of bivalves are Ca^{2+} dependent, whereas Ca^{2+}-independent lectins, such as those in *S. constricta*, have been rarely investigated [29]. The present study focused on molecular characterization and functional analysis of a novel Ca^{2+}-independent CLR from *S. constricta*. The cDNA sequence of the novel CLR gene was cloned from *S. constricta*. The temporal spatial and time-course expression profiles were investigated. The bacterial binding specificity and agglutination activities of ScCTL-2 were examined to provide evidence for understanding the multiple functions of invertebrate CTLs.

2. Materials and methods

2.1. Animal and bacterial challenge experiment

Healthy *S. constricta* clams (n = 100, 5–6 cm in length) were purchased from a commercial shellfish farm (Ninghai, Zhejiang province, China), equally divided into two tanks, and kept in similar conditions. The pathogen challenge experiments were performed according to our previous work [24]. One tank of razor clams was exposed to *V. parahaemolyticus* with a final concentration of 1.0×10^7 CFU/mL, and the other tank of razor clams was not exposed to *V. parahaemolyticus* and served as the control group. Two tissues, namely, gill and hepatopancreas, were collected at 0, 6, 12, and 24 h post-infection. Three biological replicates were obtained for each group, and the sample of each replicate was collected from three individuals in every point. All samples were preserved at −80 °C until subsequent use.

2.2. Cloning of the full-length cDNA of ScCTL

Through sequence alignment, we chose lectins with only one conserved motif for full-length amplification and function exploration from the transcriptome database. Total RNA was extracted with RNAiso Plus reagent (Takara). First-strand cDNA was synthesized according to the 3′ and 5′ full RACE core set instructions (TaKaRa). Two gene specific primers P1 and P2 (Table 1) were designed based on the annotated EST of *ScCTL-2* for 3′RACE. The desired PCR products were cloned into the pMD19-T simple vector (TaKaRa) and sequenced at Sangon Biotechnology (Shanghai). The obtained sequence was assembled using BioEdit.

2.3. Bioinformatics analysis

Sequence homology was analyzed based on the level of sequence identities between the translated nucleotide sequence of ScCTL and the protein sequences from other species by using BLAST algorithm at the National Center for Biotechnology Information (https://blast.ncbi.nlm.nih.gov/Blast.cgi). The cleavage site of the signal peptides was predicted using the SignalP 4.1 program (http://www.cbs.dtu.dk/services/SignalP/). Potential N-glycosylation sites were predicted using NetNGlyc1.0 Server (http://www.cbs.dtu.dk/services/NetNGlyc/). The potential disulfide bonds and their positions were predicted using the Scanprosite program (http://www.expasy.ch/tools/scanprosite/). Multiple sequence alignment was performed using the BioEdit program (http://clustalw.ddbj.nig.ac.jp/) based on the CRD of different original CTLs [14].

Table 1
Primers used in the present study. The underline is the restriction sites.

Primer	Sequence (5′-3′)	Position in *ScCTL-2*
3′ Adaptor primer	GGCCACGCGTCGACTAGTACTTTTT	
P1	CAACACCCAAACCTACAACAACCCC	598–622
P2	ATCTTCATGGTTACGCTCACTGGGC	406–430
P3	GGATCCTTCCTGCTTGGCAATGAAC	110–129
P4	GCGGCCGCATTACAATTGCATTCCACAC	921–941
P5	TGTCCATCAAGTGTCAGGTCCCA	138–160
P6	CTTGTCGCTCAGTCCAATCCAGA	345–368
β-actin-F	ACACTACTGAAGGCACGCTAA	
β-actin-R	ACAACGAACCAACCCAAGA	

2.4. Spatial expression of ScCTL-2 mRNA transcripts

The expression patterns of *ScCTL-2* in five different tissues, namely, gill, hepatopancreas, hemocyte, foot, and siphon, were investigated on a 7500 real-time quantitative PCR system (Thermo Fisher Scientific). β-Actin served as internal control to verify successful reverse transcription and calibrate the cDNA template (Table 1). Two specific primers P3 and P4 (Table 1) of *ScCTL-2* were designed to amplify a product of 231 bp. Real-time PCR was performed in a total reaction volume of 20 μL containing 10 μL of 2 × SYBR Green Mix (TaKaRa), 8 μL of diluted cDNA (1:20), 0.8 μL of each primer (10 mM), and 0.4 μL of ROX II. The qPCR parameters included a denaturing step at 95 °C for 2 min, followed by 40 cycles at 95 °C for 15 s, 55 °C for 20 s, and 72 °C for 45 s. The amplified products were subjected to melting analysis at the end of each PCR run to confirm the generation of a single PCR product. $2^{-\Delta\Delta CT}$ method was used to analyze the expression levels of *ScCTL-2*. The values represent n-fold difference relative to the hepatopancreas.

2.5. Time-course analysis of ScCTL-2 in response to V. parahaemolyticus challenge

Gill and hepatopancreas were selected to analyze the temporal expression profile of *ScCTL-2* in *Vibrio*-challenged samples from Section 2.1. RNA extraction, cDNA synthesis, and expression analysis were performed according to methods in Section 2.2. The untreated samples served as the control (calibrator). The values obtained denoted n-fold differences relative to the calibrator. Data are presented as mean ± SD (n = 3). The results were subjected to one-way ANOVA followed by Duncan's multiple range tests to determine differences between the challenged and control groups at each sampling time. P values less than 0.05 were considered significantly different.

2.6. Prokaryotic expression and purification of recombinant ScCTL-2

The mature peptide of ScCTL-2 was amplified from cDNA by using the primers of P5 and P6 (Table 1). After restriction enzyme digestion, the product was orientally inserted into the same digested pET-28a (+) vector. The recombinant pET-28a-ScCTL-2 plasmid was transformed into competent *Escherichia coli* BL21 cells. The recombinant ScCTL-2 was generated by adding IPTG with a final concentration of 0.2 mM and purified using a nickel-nitrilotriacetic acid (NiNTA) column (QIAGEN, Hilden, Germany). The purified protein was confirmed by sodium dodecyl sulfate polyacrylamide gel electrophoresis (SDS-PAGE) under reducing conditions and visualized using Coomassie bright blue R250.

2.7. Antiserum preparation

For polyclonal antibody preparation, the purified proteins were loaded into wells of 12% SDS polyacrylamide gels. Electrophoresis was carried out on a Bio-Rad mini-gel apparatus at room temperature by using 1 × Tris-Glycine buffer [0.025 M Tris, 0.25 M Glycine, 0.1% (w/v) SDS]. The target protein was obtained using 0.25 mM KCl solution, cut into small strips, and ground with PBS. A 4-week-old mouse was intradermally injected with a mixture containing 100 μg of the purified ScCTL-2. The mouse was boosted twice with 75 and 50 μg of the protein

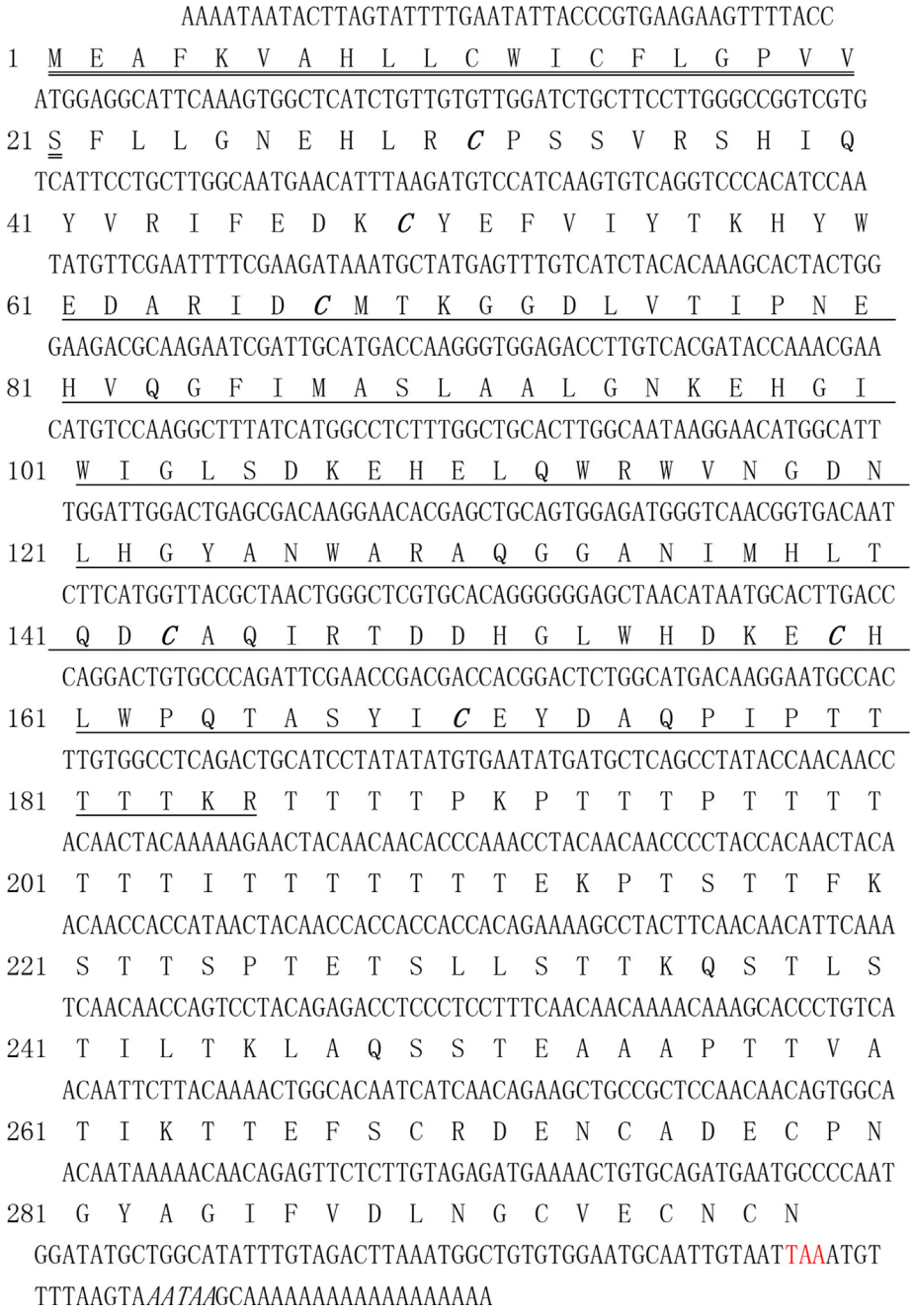

Fig. 1. The nucleotide and deduced amino acid sequence of ScCTL-2. The putative signal peptide and the CRD region of ScCTL-2 were double-and single-underlined, respectively. The conserved "W*D″ motif was shadowed, and cysteines were shown in bold italics.

at 1-week interval. One week after the last immunization, the antiserum was harvested from mouse eyes and stored at −80 °C until further use.

2.8. Bacterial binding activity analysis

Three Gram-negative bacterial species, namely, *E. coli*, *Vibro anguillarum*, and *V. parahaemolyticus*, and Gram-positive *M. luteus* were cultured and used in the assay to detect the bacterial binding activities of rScCTL-2. Based on a previous method [30], the bacteria were incubated with ScCTL-2 (50 μg) for 1 h at room temperature with shaking after washing with TBS (10 mM Tris-HCl, 150 mM NaCl, pH 7.5) or TBS-Ca^{2+} (TBS, 5 mM $CaCl_2$). The pelleted bacteria were used to detect the bacterial binding activity by Western blot analysis. TBS without rScCTL-2 and recombinant protein (50 μg) were used as negative and positive controls, respectively. Mouse anti-ScCTL-2 antiserum from Section 2.7 was used as the primary antibody at 1:400 dilution, and horseradish peroxidase (HRP, Beyotime)-labeled goat anti-mouse IgG (1:3000) was used as the secondary antibody. The membrane was washed and incubated in Western Lightning-ECL substrate (Perkin Elmer) prior to exposure onto X-OMAT AR X-ray film (Eastman Kodak, Rochester, NY).

2.9. Bacteria agglutination assay

We also used the four bacterial species mentioned in the agglutinating assay according to a previously described method [31]. The bacterial suspension was added with fluorescein isothiocyanate (FITC, with final concentration of 100 μg/ml, Solarbio, China) dissolved in DMSO and incubated at room temperature for 2 h. The suspension was then incubated with 500 μL of ScCTL-2 (1 μg/μL) and fluorescent

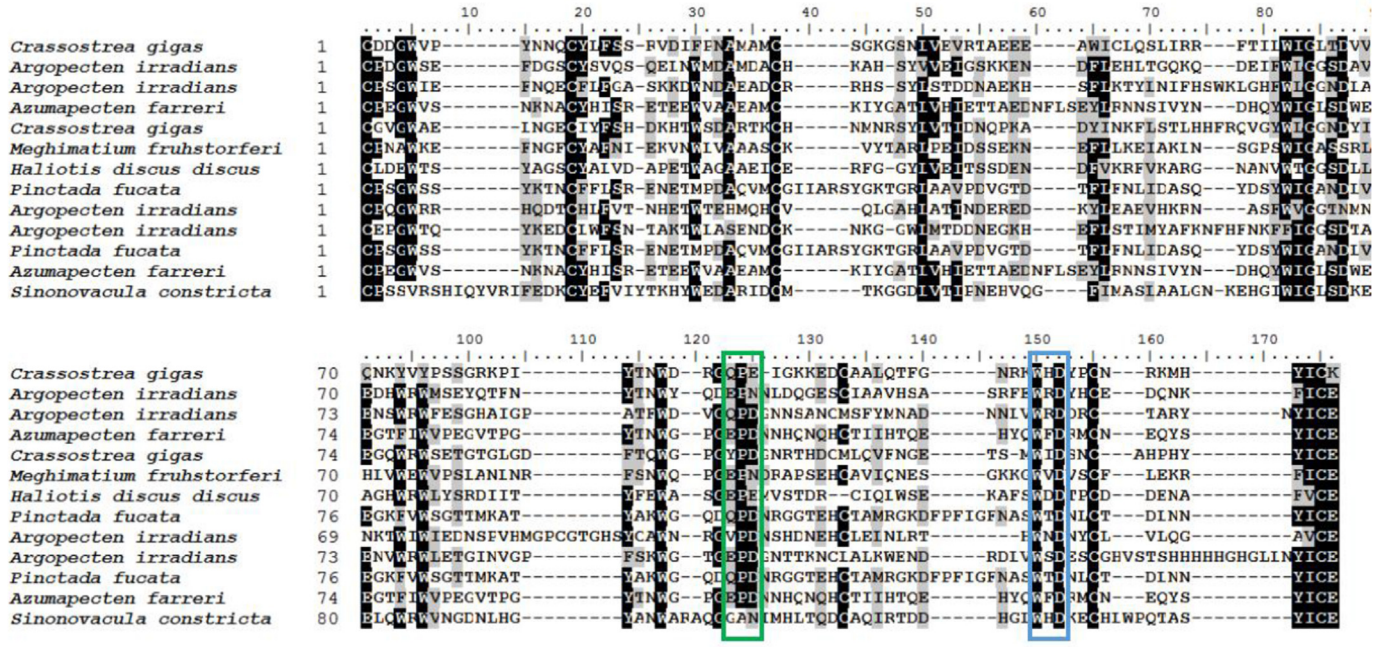

Fig. 2. Multiple alignment of the CRD sequences of ScCTL and CRDs from other lectins. Threshold for shading is > 60%, and similar residues are marked with gray shading; identical residues are marked with black shading. The first and second motif is boxed in green and blue. (For interpretation of the references to colour in this figure legend, the reader is referred to the Web version of this article.)

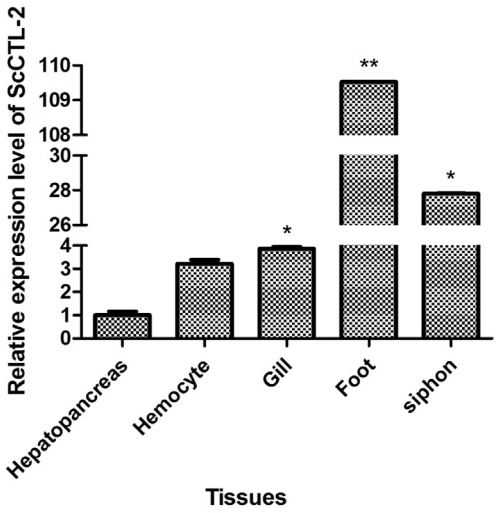

Fig. 3. Tissue distribution of the *ScCTL-2* transcript was detected via qRT-PCR. mRNA expression levels in the hemocyte, gill, foot, and siphon were normalized to that in hepatopancreas. Values are given as mean ± S.D (n = 3). Asterisks indicate significant differences (*P < 0.05, **P < 0.01).

bacteria at room temperature for 1 h with TBS-Ca^{2+} (10 mM Tris-HCl, 150 nm NaCl, 10 mM $CaCl_2$, pH 7.5) and with or without EDTA (10 mM, chelating agents). BSA-Ca^{2+} and TBS served as negative and blank controls. A total of 10 μL of the coincubation solution was added onto the glass slides to observe agglutination by fluorescence microscopy (NiKon, camera: Eclipse TS100, scope: Eclipse TI-U).

3. Results

3.1. Sequence analysis of ScCTL-2

The nucleotide sequence of *ScCTL-2* cDNA was deposited in the GenBank under the accession number MF289977. The full-length cDNA of *ScCTL-2* comprised a 5′ UTR of 47 bp, a 3′ UTR of 37 bp, and a putative ORF of 894 bp encoding 298 amino acid residues (Fig. 1) with a predicted weight of 33.16 kDa and a theoretical pI of 5.71. The protein was predicted to have a 21 amino acid residues signal peptide (Fig. 1) and has an identity of 39% (E-value = 2e-36) with *Haliotis discus hannai*. A characteristic CRD domain was detected from Cys^{31} to Glu^{171} in the deduced amino acid of ScCTL-2 (Fig. 2). Eight cysteine residues forming four couple of intramolecular disulfide bonds (Cys^{44}-Cys^{62}, Cys^{80}-Cys^{310}, Cys^{156}-Cys^{183}, and Cys^{172}-Cys^{305}) were also totally conserved in ScCTL-2. Multiple sequence alignment showed that ScCTL-2 had a Ca^{2+}-binding motif "W*D" (Fig. 2), which was conserved in other mollusk CRDs. The other one was not found in the first motif location.

3.2. Spatial expression analysis of ScCTL-2 mRNA

The spatial mRNA expression pattern of *ScCTL-2* in the different tissues is shown in Fig. 3. *ScCTL-2* transcripts were detected in all tested tissues including hepatopancreas, gill, hemocyte, siphon, and foot. The highest expression level was detected in foot, followed by siphon and gill. Hepatopancreas displayed the lowest expression level in all five tissues (Fig. 3).

3.3. ScCTL-2 expression upon V. parahaemolyticus challenge in gills and hepatopancreas

The temporal expression of *ScCTL-2* transcripts in the hepatopancreas and gill after *V. parahaemolyticus* challenges is shown in Fig. 4. The mRNA level of *ScCTL-2* in the gill was significantly upregulated at the first 6 h ($P = 0.020$) and reached its peak expression at 12 h with a 4.40-fold increase ($P = 0.032$) compared with the control group. Afterwards, although a downregulated expression of *ScCTL-2* was detected at 24 h ($P = 0.019$), the expression level was still higher than the control group ($P < 0.05$). In the hepatopancreas, the expression level of *ScCTL-2* was sharply increased at 6 h and maintained at this level at until 12 h by 3.35-folds ($P = 0.003$) compared with the control group, whereas no significant difference was detected in other time points (Fig. 4).

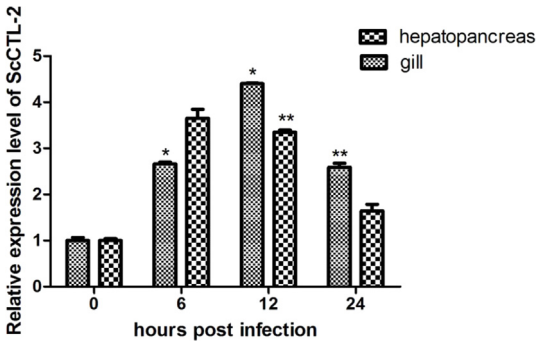

Fig. 4. Expression levels of *ScCTL-2* in the hepatopancreas and gill after *V. parahaemolyticus* infection. Three biological replicates were conducted in the experiment, and the data are showed as the mean ± S.D (n = 3). Asterisks indicate significant differences (*P < 0.05, **P < 0.01).

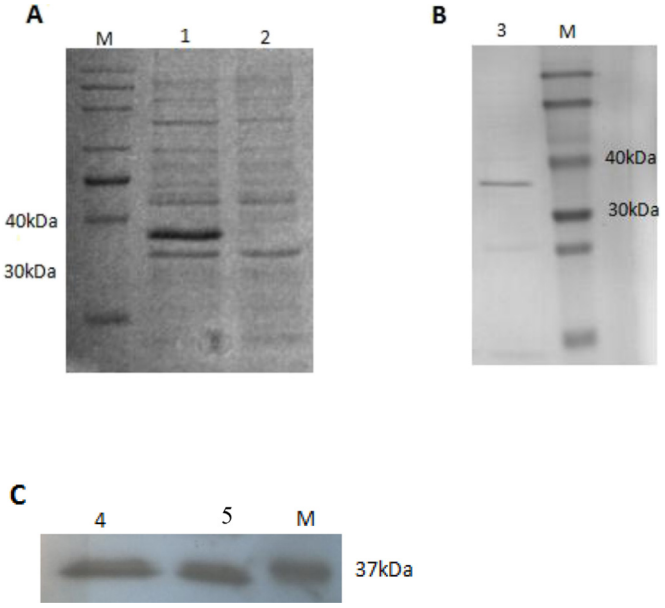

Fig. 5. The induction (A) and purification (B) of recombinant ScCTL-2 protein. The polyclonal antibody against ScCTL-2 was prepared based on the obtained ScCTL-2 protein, and the specificity of the antibody was detected via Western blot (C). Lane M: protein weight marker; line 1: ScCTL-2 protein was induced for 7 h by IPTG through recombinant pET28a-ScCTL-2 via BL21; line 2: The blank pET28a was served as a negative control and also induced with IPTG; line 3: A band with no miscellaneous proteins was obtained by the purification of rScCTL-2 protein; line 4: Purified protein as positive control was used to detect antibody singularity; line 5: Total protein was used to detect antibody singularity.

Fig. 6. Bacteria-binding activities of rScCTL-2 were assayed in the presence (A) and absence (B) of Ca^{2+}, respectively. In this study, we used each bacterium with a number of 1.0×10^5 CFU to detect the bacteria-binding activity of ScCTL-2 by adding sufficient amount of rScCTL-2. Positive and negative controls were set by adding equal amount of rScCTL-2 (50 μg) and TBS, respectively. In this figure, *V.p.*: *V. parahaemolyticus*; *V.a*: *V. anguillarum*; *E.c*: *E.coli*; *M.l*: *M. luteus.*

3.4. Protein-purified and antibody-prepared rScCTL-2

After IPTG induction, one major protein with an apparent molecular weight of 38 kDa was detected in the positive transformant (Fig. 5A), which could be further purified to homogeneity by using NiNTA column (Fig. 5B). The protein was then used for antibody preparation of rScCTL-2. Western blot verification showed that the prepared antibody could specifically bind to the recombinant protein and total protein (Fig. 5C).

3.5. Bacteria-binding activity of rScCTL-2

As shown in Fig. 6, rScCTL-2 exhibited binding activity towards all gram-negative (*E. coli*, *V. anguillarum*, and *V. parahaemolyticus*) bacteria but not gram-positive (G^+, *M. luteus*) bacteria whether in the absence of Ca^{2+} or not. Among them, ScCTL-2 exhibited stronger binding activity against *E.coli* compared with other two G^- bacteria. Although Ca^{2+} was not a determinant factor in the binding assay, the binding capacities could be enhanced after Ca^{2+} supplementary.

3.6. Bacteria-agglutinating assay of rScCTL-2

The results showed that rScCTL-2-Ca^{2+} could agglutinate G^- bacteria with or without EDTA, but the latter displayed a greater agglutinated activity. rScCTL-2 could induce a stronger level of aggregation of *E. coli* than that of other G^- bacteria (Fig. 7A–C). However, rScCTL-2-Ca^{2+} had no agglutinating activities to *M. luteus* with the presence of EDTA or not (Fig. 7D).

4. Discussion

The high mortality caused by bacteria is an important limitation for the development of *S. constricta* aquaculture [3]. The innate immune system is a fundamental defense mechanism for invertebrates [4]. Among this system, CLRs, which serve as one of PRRs, bind to the glycan structures of pathogens and activate the innate immune system by recognizing pathogenic PAMPs [32]. In each CRD, a typical double-loop stabilized by three or two pairs of disulfide bridges and four Ca^{2+}-binding sites are present, among which the Ca^{2+}-binding site 2 is believed to be essential to the recognition of carbohydrate ligand [33]. One binding site W*D motif was found in ScCTL-2. All these characterizations suggested that ScCTL-2 should be a new member of C-type lectin and may be involved in immune response against bacterial challenge.

CTLs have broad distributions in multiple tissues [34,35]. *Lec-2* from *Chlamys Farreri* was detected in mantle, which is an important organ located inside shells, covering the surface of the mollusk to contact most frequently with pathogens [36]. Its high expression level might be explained as follows: the mantle was the first barrier to probably recognize pathogen during filter-feeding or movement in seawater. In this study, the *ScCTL-2* mRNA transcript was distributed mainly in the foot and siphon, which was consistent with the reports in *Haliotis discus* [23]. We infer that the foot and siphon are involved in a continuous water exchange and food uptake from the outside environment. Recent studies in *Crassostrea virginica* have also shown that lectins are associated with food intake and support this result [15].

To confirm whether or not CTLs are involved in immune response, transcript profile expression levels of CTLs in immune organs were conducted in some marine species [37–39]. As the primary immune organs, the gills and hepatopancreas play very important roles in the immune response of host and were often used to explore the biological functions on immune defense [3]. In this study, the transcript profiles of *ScCTL-2* in the hepatopancreas and gills were both upregulated (Fig. 3) at 6 h after challenging with *V. parahaemolyticus*. Similarly, the expression levels of *PcLec6* in gills were upregulated after challenging with *V. alginolyticus* [40]. *VpCTL* in the hepatopancreas after *Listonella*

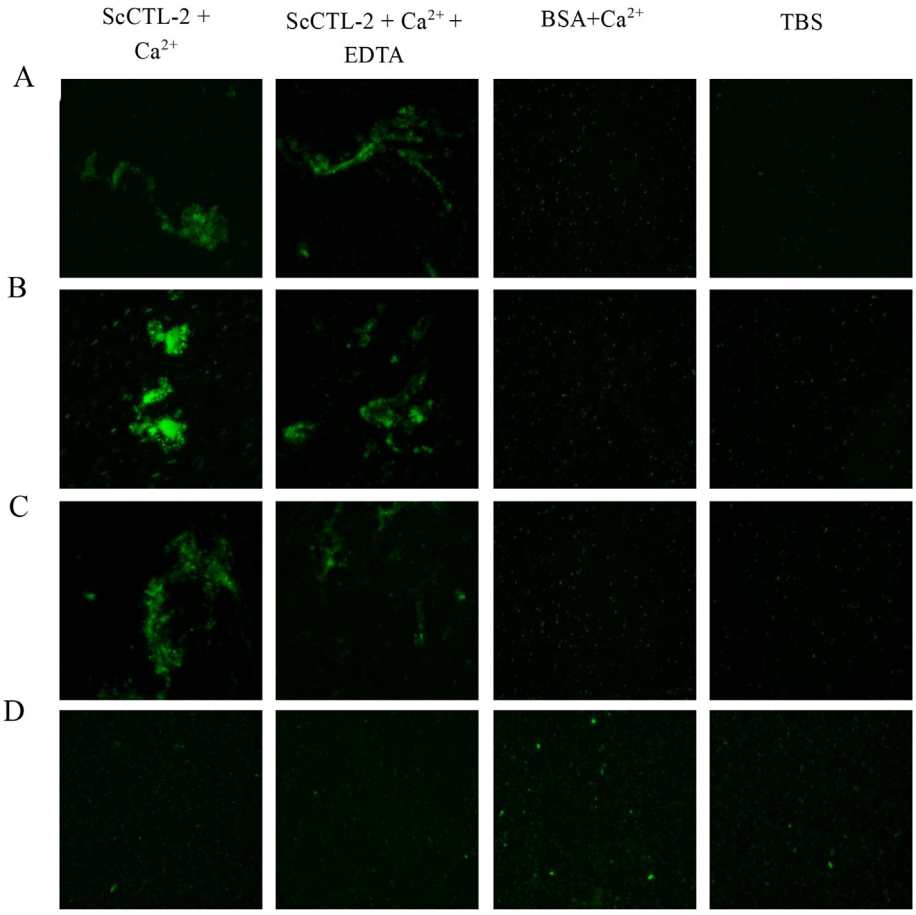

Fig. 7. Bacterial agglutination assay of rScCTL-2. (A) *V. parahaemolyticus*. (B) *E. coli*. (C) *V. anguillarum*. (D) *M. luteus*. The magnification of the microscope is 40×.

anguillarum challenging had the highest expression [41]. The mRNA expression profiles of *ScCTL-2* post *V. parahaemolyticus* stimulation suggested it was inducible expression to exert an important function in the immune response of *S. constricta* against pathogen infection.

Ca^{2+} had been confirmed to be an important factor for binding microorganisms of CTLs. For instance, CTL-S3 [25] and TfCTL1 [42] bind to several kinds of microorganisms selectively in a Ca^{2+}-dependent manner. Agglutination is also the dominant function for lectins to interact and eliminate bacteria [43,44]. Many lectins have different agglutination activities for different types of microorganisms, such as *Staphylococcus aureus* [25], *V. anguillarum* [14], and yeast [45]. In our results, rScCTL-2 could bind and agglutinate to all G^- bacteria with or without Ca^{2+} (Figs. 6,7A-C). The capacity was enhanced by Ca^{2+} supplementation, which was coincident with some reported studies [37,46]. In *Eriocheir sinensis*, EsLecD exhibited the ability to bind and agglutinate to all tested microorganisms in a Ca^{2+}-independent manner, and its binding affinity increased significantly with the presence of Ca^{2+} toward microorganisms [47]. This result was consistent with our structure analysis, which indicated that "WHD," as a calcium binding site, could enhance the ability of binding bacteria in *S. constricta* (Fig. 2). However, rScCTL-2 has no effect on *M. luteus*, whether Ca^{2+} was present or not (Figs. 6 and 7D), which was consistent with the fact that G^- bacteria was the major pathogen for clam disease outbreak [3]. The binding and agglutinating spectrum of rScCTL-2 suggested that it has important roles in the immune defense against G^- bacteria in *S. constricta*, such as the common pathogen *Vibrio*. The same results were reflected in Cflec-1 from *C. Farreri* [48] and rAiCTL5 from *Argopecten irradians* [49]. The identification of bacteria via CTLs is mainly due to differences in cell wall composition [50]. Although many experiments have shown that CTLs recognize different bacteria and also bind to specific PAMPs [51], some experiments show that AiCTL-3 bound to peptidoglycans from G^+ bacteria only binds with *S. aureus* but not with *Bacillus subtilis* and *M. luteus* [52]. This characteristic may be due to the tiny difference in the cell wall composition of G^- bacteria [53]. This result indicates that rScCTL-2 is sensitive to different G^- bacteria and trigger different immune signals. Agglutination and binding experiments have shown that rScCTL-2 may be used as a specific immune factor of G^- bacteria in *S. constricta*, which has guiding significance in the aquaculture industry.

Notes

The authors declare no competing financial interest.

Acknowledgments

This work was financially supported by Zhejiang Major Program of Science and Technology (2016C02055-9), Natural Science Foundation of Ningbo (2015C10009), Fund from Ningbo University for Xuelin Zhao (XYL17010), and the K.C. Wong Magna Fund in Ningbo University.

References

[1] S. Xie, D. Niu, R. Haideng, et al., Molecular characterization of IGFBP and association analysis with growth traits in the razor clam *Sinonovacula constricta*, J. Fish. China 06 (2015).
[2] M. Peng, D. Niu, Z. Chen, et al., Expression of a novel complement C3 gene in the razor clam *Sinonovacula constricta*, and its role in innate immune response and hemolysis, Dev. Comp. Immunol. 73 (2017) 184.
[3] X. Zhao, X. Duan, Z. Wang, et al., Comparative transcriptome analysis of *Sinonovacula constricta* in gills and hepatopancreas in response to *Vibrio parahaemolyticus* infection, Fish Shellfish Immunol. 67 (2017) 523–535.

[4] L. Song, L. Wang, H. Zhang, et al., The immune system and its modulation mechanism in scallop, Fish Shellfish Immunol. 46 (1) (2015) 65–78.
[5] X.Q. Yu, Y.F. Zhu, C. Ma, et al., Pattern recognition proteins in *Manduca sexta* plasm, Insect Biochem. Mol. Biol. 32 (10) (2002) 1287–1293.
[6] X.W. Wang, J.X. Wang, Pattern recognition receptors acting in innate immune system of shrimp against pathogen infections, Fish Shellfish Immunol. 34 (4) (2013) 981–989.
[7] X.Z. Shi, X.Q. Yu, The extended loop of the C-terminal carbohydrate-recognition domain of *Manduca sexta* immulectin-2 is important for ligand binding and functions, Amino Acids 42 (6) (2012) 2383–2391.
[8] X.W. Wang, X.F. Zhao, J.X. Wang, C-type lectin binds to β-integrin to promote hemocytic phagocytosis in an invertebrate, J. Biol. Chem. 34 (6) (2013) 2405-2014.
[9] J.L. Yang, L.L. Wang, H. Zhang, et al., C-type lectin in *Chlamys farreri* (CfLec-1) mediating immune recognition and opsonization, PloS One 6 (2) (2011) e17089.
[10] L.L. Wang, L.L. Wang, J.L. Yang, A multi-CRD C-type lectin with broad recognition spectrum and cellular adhesion from *Argopectenirradians*, Dev. Comp. Immunol. 36 (3) (2012) 591–601.
[11] H. Jiang, Y.M. Cai, L.Q. Chen, et al., Functional annotation and analysis of expressed sequence tags from the hepatopancreas of mitten crab (*Eriocheir sinensis*), Mar. Biotechnol. 11 (3) (2009) 317–326.
[12] H.Z. Guo, P.F. Zou, J.P. Fu, et al., Characterization of two C-type lectin-like domain (CTLD)-containing proteins from the cDNA library of Chinese mitten crab *Eriocheir sinensis*, Fish Shellfish Immunol. 30 (2) (2011) 515–524.
[13] H. Sun, X.U. Xiao-Yong, X.L. Tian, et al., Activation of NF-kB and respiratory burst following Aspergillus fumigatus stimulation of macrophages, Immunobiology 219 (1) (2014) 25–36.
[14] H. Li, H. Zhang, S. Jiang, et al., A single-CRD C-type lectin from oyster *Crassostrea gigas* mediates immune recognition and pathogen elimination with a potential role in the activation of complement system, Fish Shellfish Immunol. 44 (2) (2015) 566–575.
[15] E.E. Pales, B. Allam, Reverse genetics demonstrate the role of mucosal C-type lectins in food particle selection in the oyster *Crassostrea virginica*, J. Exp. Biol. 221 (pt6) (2018).
[16] S.E. Hardison, G.D. Brown, C-type lectin receptors orchestrate antifungal immunity, Nat. Immunol. 13 (9) (2012) 817–822.
[17] Y. Xiu, Y. Wang, J. Bi, et al., A novel C-type lectin is involved in the innate immunity of *Macrobrachium nipponense*, Fish Shellfish Immunol. 50 (2016) 117–126.
[18] L. Wang, L. Wang, M. Huang, et al., The immune role of C-type lectins in molluscs, Invertebr. Surviv. J. 8 (2) (2011) 241–246.
[19] A. Zhang, Y. Lu, C. Li, et al., A small heat shock protein (sHSP) from *Sinonovacula constricta*, against heavy metals stresses, Fish Shellfish Immunol. 34 (6) (2013) 1605–1610.
[20] T.B.H. Geijtenbeek, S.I. Gringhuis, Signalling through C-type lectin receptors: shaping immune responses, Nat. Rev. Immunol. 9 (7) (2009) 465–479.
[21] H. Zhang, H. Wang, L. Wang, et al., A novel C-type lectin (Cflec-3) from *Chlamys farreri* with three carbohydrate-recognition domains, Fish Shellfish Immunol. 26 (5) (2009) 707–715.
[22] J.C. Hoving, G.J. Wilson, G.D. Brown, Signalling C-type lectin receptors, microbial recognition and immunity, Cell Microbiol. 16 (2) (2014) 185–194.
[23] N. Wang, I. Whang, J. Lee, A novel C-type lectin from abalone, *Haliotis discus discus*, agglutinates *Vibrio alginolyticus*, Dev. Comp. Immunol. 32 (9) (2008) 1034–1040.
[24] P. Kong, L. Wang, H. Zhang, et al., A novel C-type lectin from bay scallop *Argopecten irradians* (AiCTL-7) agglutinating fungi with mannose specificity, Fish Shellfish Immunol. 30 (3) (2011) 836–844.
[25] M.Y. Zhan, T. Shahzad, P.J. Yang, et al., A single-CRD C-type lectin is important for bacterial clearance in the silkworm, Dev. Comp. Immunol. 65 (2016) 330–339.
[26] S.T. Iobst, K. Drickamer, Binding of sugar ligands to Ca^{2+}-dependent animal lectins. II. Generation of high-affinity galactose binding by site-directed mutagenesis, J. Biol. Chem. 269 (22) (1994) 15512–15519.
[27] J. Yang, M. Huang, H. Zhang, et al., CfLec-3 from scallop: an entrance to non-self recognition mechanism of invertebrate C-type lectin, Sci. Rep. 5 (2015) 10068.
[28] J. Yang, L. Wang, H. Zhang, et al., C-Type Lectin in *Chlamys farreri* (CfLec-1) Mediating Immune Recognition and opsonization, PloS One 6 (2) (2011) e17089.
[29] Y. Shen, Y. Shao, Y. Cui, et al., Novel C-type lectin from razor clam *Sinonovacula constricta* agglutinates bacteria and erythrocytes in a Ca^{2+}-dependent manner, Dev. Comp. Immunol. 86 (2018) 9–16.
[30] K. Ono, T.A. Suzuki, Y. Toyoshima, et al., SJL-1, a C-type lectin, acts as a surface defense molecule in Japanese sea cucumber, *Apostichopus japonicus*, Mol. Immunol. 97 (2018) 63–70.
[31] Y. Guan-Jun, L. Xin-Jiang, C. Qiang, et al., Molecular characterization and functional analysis of a novel C-type lectin receptor-like gene from a teleost fish, *Plecoglossus altivelis*, Fish Shellfish Immunol. 44 (2) (2015) 603–610.
[32] M. Huang, X. Song, J. Zhao, et al., A C-type lectin (AiCTL-3) from bay scallop *Argopecten irradians*, with mannose/galactose binding ability to bind various bacteria[J], Gene 531 (1) (2013) 31–38.
[33] A.N. Zelensky, J.E. Gready, The C-type Lectin-like Domain Superfamily - Zelensky - 2005, FEBS Journal - Wiley Online Library. Febs Journal, 2005.
[34] X.B. Bao, C.B. He, C.D. Fu, et al., A C-type lectin fold gene from Japanese scallop *Mizuhopecten yessoensis*, involved with immunity and metamorphosis, Genet. Mol. Res. 14 (1) (2015) 2253–2267.
[35] K. Yamaura, K.G. Takahashi, T. Suzuki, Identification and tissue expression analysis of C-type lectin and galectin in the Pacific oyster, *Crassostrea gigas*, Comp. Biochem. Physiol., B 149 (1) (2008) 168–175.
[36] J. Yang, L. Qiu, X. Wei, et al., An ancient C-type lectin in *Chlamys farreri* (CfLec-2) that mediate pathogen recognition and cellular adhesion, Dev. Comp. Immunol. 34 (12) (2010) 1274.
[37] X.H. Zhang, Y.H. Shi, J. Chen, Molecular characterization of a transmembrane C-type lectin receptor gene from ayu (*Plecoglossus altivelis*) and its effect on the recognition of different bacteria by monocytes/macrophages, Mol. Immunol. 66 (2) (2015) 439–450.
[38] C. Mu, L. Chen, J. Zhao, et al., Molecular cloning and expression of a C-type lectin gene from *Venerupis philippinarum*, Mol. Biol. Rep. 41 (1) (2014) 139–144.
[39] A. Jingqun, D. Yang, C. Yuanyuan, et al., Molecular characterization and biological effects of a C-type lectin-like receptor in large yellow croaker (*Larimichthys crocea*), Int. J. Mol. Sci. 16 (12) (2015) 29631–29642.
[40] X.W. Zhang, X. Man, X. Huang, et al., Identification of a C-type lectin possessing both antibacterial and antiviral activities from red swamp crayfish, Fish Shellfish Immunol. 77 (2018) 22–30.
[41] C. Mu, L. Chen, J. Zhao, et al., Molecular cloning and expression of a C-type lectin gene from *Venerupis philippinarum*, Mol. Biol. Rep. 41 (1) (2014) 139–144.
[42] S. Yu, H. Yang, Y. Chai, et al., Molecular cloning and characterization of a C-type lectin in roughskin sculpin (*Trachidermus fasciatus*), Fish Shellfish Immunol. 34 (2) (2013) 582–592.
[43] W.K. Eddie Ip, K. Takahashi, R. Alan Ezekowitz, et al., Mannose-binding lectin and innate immunity, Immunol. Rev. 230 (1) (2009) 9–21.
[44] J. Lu, Z. Yu, C. Mu, et al., Characterization and functional analysis of a novel C-type lectin from the swimming crab *Portunus trituberculatus*, Fish Shellfish Immunol. 64 (2017) 185–192.
[45] Y. Yu, Y. Yu, H. Huang, et al., A short-form C-type lectin from amphioxus acts as a direct microbial killing protein via interaction with peptidoglycan and glucan, J. Immunol. 179 (12) (2007) 8425.
[46] H. Yang, T. Luo, F. Li, et al., Purification and characterisation of a calcium-independent lectin (PjLec) from the haemolymph of the shrimp *Penaeus japonicus*, Fish Shellfish Immunol. 22 (1) (2007) 88–97.
[47] X.N. Guo, X.K. Jin, S. Li, et al., A novel C-type lectin from *Eriocheir sinensis*, functions as a pattern recognition receptor with antibacterial activity, Fish Shellfish Immunol. 35 (5) (2013) 1554–1565.
[48] H. Wang, L. Song, C. Li, et al., Cloning and characterization of a novel C-type lectin from Zhikong scallop *Chlamys farreri*, Mol. Immunol. 44 (5) (2007) 722–731.
[49] C. Mu, X. Song, J. Zhao, et al., A scallop C-type lectin from *Argopecten irradians* (AiCTL5) with activities of lipopolysaccharide binding and Gram-negative bacteria agglutination, Fish Shellfish Immunol. 32 (5) (2012) 716–723.
[50] M. Huang, C. Mu, Y. Wu, et al., The functional characterization and comparison of two single CRD containing C-type lectins with novel and typical key motifs from *Portunus trituberculatus*, Fish Shellfish Immunol. 70 (2017) 398–407.
[51] X.W. Zhang, W.T. Xu, X.W. Wang, et al., A novel C-type lectin with two CRD domains from Chinese shrimp *Fenneropenaeus chinensis* functions as a pattern recognition protein, Mol. Immunol. 46 (8) (2009) 1626–1637.
[52] M. Huang, X. Song, J. Zhao, et al., A C-type lectin (AiCTL-3) from bay scallop *Argopecten irradians*, with mannose/galactose binding ability to bind various bacteria, Gene 531 (1) (2013) 31.
[53] M.A. Anwar, S. Choi, Gram-negative marine bacteria: structural features of lipopolysaccharides and their relevance for economically important diseases, Mar. Drugs 12 (5) (2014) 2485–2514.